DOI: 10.1002/ejic.201100534

1D Co^{II} and Ni^{II} Chiral Polymers That Exhibit Ferromagnetic Interactions

Ghenadie Novitchi,[a,b] Guillaume Pilet,[a] and Dominique Luneau*[a]

Keywords: Crystal engineering / Chain structures / Cobalt / Nickel / Carboxylate ligands

Four transition-metal coordination compounds with D- and L-mandelic acid (H*mand*) were synthesized and structurally and magnetically characterized. The structure, refined as $\{M^{II}(L/D\text{-}mand)(4\text{-}MePy)_3\}_n{\cdot}n(ClO_4)$ (M = Co^{II} and Ni^{II}; 4-MePy = 4-methylpyridine), reveals a chiral 1D polymer that consists of a chain complex built by the monocarboxylate ligand. The coordination sphere of the paramagnetic center is chiral and completed by three 4Me–Py ligands. Magnetic studies reveal the presence of a ferromagnetic interaction between the Ni^{II} centers [J = 0.64(5)–0.54(7) cm^{-1} and zero-field splitting (ZFS) = –1.38(1)/–1.05(2) cm^{-1}]. In the case of the Co^{II}-based polymer, ferromagnetic but negligible interaction is suspected.

Introduction

Crystal engineering of structures that possess various network topologies attracts much attention due to their potential applications in many important fields such as catalysis, hydrogen storage, metal–organic frameworks, electrical conductivity, and molecular magnets.[1–11] Among these, coordination polymers are an important class of engineered structures. In this case, the strategies for the synthesis of one-dimensional (1D), two-dimensional (2D), or three-dimensional (3D) frameworks often take advantage not only of coordination bonding but also of other directional interactions such as versatile hydrogen-bonding,[12,13] π–π-stacking,[13,14] and electrostatic interactions.[15–17]

To obtain polymeric structures, a large variety of ligands have been used. By contrast, chiral ligands remain underexplored, particularly in the design and preparation of an acentric arrangement. In the field of molecular magnetic materials, asymmetric ligands may be used to induce an asymmetric environment of paramagnetic centers and/or a non-centrosymmetric repartition of paramagnetic centers along the polymers and also in crystal packing. Such non-centrosymmetric repartition of the spin carriers can greatly affect the bulk magnetic properties of the material as has been shown in some 1D coordination systems of metal with chiral nitroxide radical.[18–21] This might even give rise to new phenomena such as magnetochiral dichroism (MCD) and chiral wave propagation. In that context, high MCD has been recently observed in chiral Cr^{III} compounds.[22,23]

With these ideas in mind, we focused our attention on the possibility of developing new chiral coordination polymers that involve bivalent ions. Mandelic acid, H*mand*, was selected because it possesses different coordination modes[24–35] (see Scheme 1) and is a good candidate to elaborate new enantiopure 1D coordination polymers. Meanwhile, the introduction of a second type of an intermetal center bridge such as azide, N_3^-, as the magnetic relay between chiral chains was considered to favor the formation of 2D chiral complexes with original magnetic behavior.

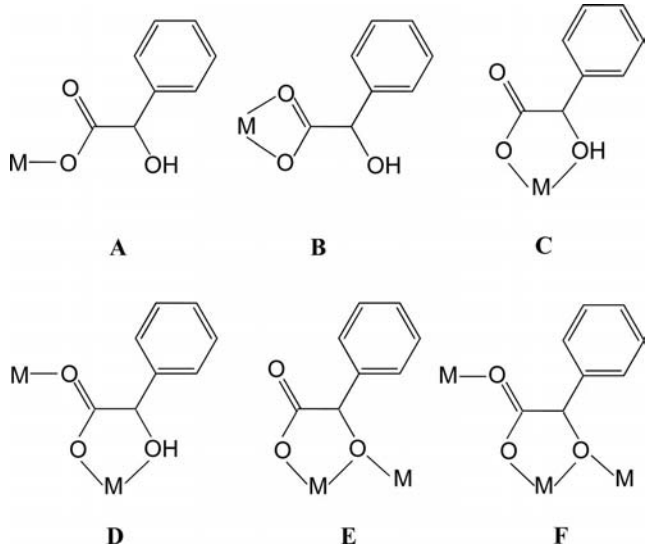

Scheme 1. Reported coordination modes for mandelic acid: **A**,[24,25] **B**,[26] **C**,[25,27,28] **D**,[29–31] **E**,[32–34] and **F**.[35]

In this paper, we report the result of a synthetic procedure with different metal ions (Mn^{II}, Co^{II}, Ni^{II}, and Cu^{II}). With Ni^{II} and Co^{II}, new 1D enantiopure polymers were crystallized as: $\{M^{II}(L\text{-}mand)(4\text{-}MePy)_3\}_n{\cdot}n(ClO_4)$ [M

[a] Université Claude Bernard Lyon 1,
Laboratoire des Multimatériaux et Interfaces (UMR 5615),
Domaine Scientifique de La Doua,
69622 Villeurbanne Cedex, France
E-mail: luneau@univ-lyon1.fr
[b] Institute of Chemistry, Academy of Sciences of Moldova,
Academiei str. 3., 2028 Chisinau, Moldova
Supporting information for this article is available on the WWW under http://dx.doi.org/10.1002/ejic.201100534.

= Co: $\mathbf{I_L}$(Co); M = Ni: $\mathbf{I_L}$(Ni); 4-MePy = 4-methylpyridine] and $\{M^{II}$(D-*mand*)(4-MePy)$_3\}_n \cdot n(ClO_4)$ [M = Co: $\mathbf{I_D}$(Co); M = Ni: $\mathbf{I_D}$(Ni)]. Their crystal structures and the results of circular dichroism and magnetic studies are reported here. Optical studies showed that we obtained the sole enantiopure compounds for all. Additionally, magnetic studies revealed ferromagnetic interactions between metal centers.

Results and Discussion

Chiral mandelic acid (L/D-H*mand*) was introduced to elaborate magnetic chiral 1D polymer complexes. It has been already reported in the literature that the asymmetry of ligands can induce an asymmetry in the environment of the paramagnetic centers and/or a non-centrosymmetric repartition of the paramagnetic centers along the polymers and within the crystal packing.[36–38] Azide salt was then used with a view to connecting these chains in 2D chiral polymers because the N_3^- bridge is known to be a good magnetic bridge between metal centers.

Addition of an excess amount of 4-MePy to a solution of chiral mandelic acid (L/D-H*mand*) in methanol mixed with $M(ClO_4)_2 \cdot 6H_2O$ (M^{II} = Cu, Mn, Co, and Ni) and NaN_3 in an equimolar ratio gave different compounds depending on the metal ion. In the case of Ni^{II} and Co^{II}, it was possible to isolate the two 1D chiral compounds $\{M^{II}$(L-*mand*)(4-MePy)$_3\}_n \cdot n(ClO_4)$ and $\{M^{II}$(D-*mand*)(4-MePy)$_3\}_n \cdot n(ClO_4)$ ($M = Ni^{II}$ or Co^{II}) starting from either L- or D-H*mand* ligands.

Complexes Based on Copper(II) Ion

With this synthetic procedure, it was impossible to isolate any complex that contained the mandelic ligand. Under all conditions, we obtained a blue viscous oil to give in the end a blue homogeneous film. From this we isolated a few crystals of a binuclear complex and some crystals of a mononuclear complex with the following refined formula obtained by single-crystal X-ray diffraction: $[Cu_2(\mu\text{-}N_3)(4\text{-MePy})_8(H_2O)_2](ClO_4)_3(4\text{-MePy})_4$ (**III**) and $[Cu(4\text{-MePy})_4(ClO_4)_2]$ (**IV**) (see the Supporting Information). As can be seen, both contain no mandelic acid.

Complexes Based on Manganese(II) Ion

Under the same conditions, a white crystalline compound was formed. According to elemental analyses and IR spectra, it corresponds to manganese(II) dimandelates $\{[Mn^{II}$(L-*mand*)$_2]$ (**V**); see the Supporting Information} that have already been reported.[29–31] This result is probably due to the best affinity of Mn^{II} ions for the oxygen environment instead of nitrogen.[39] Changing the reacting salt from $Mn^{II}(ClO_4)_2 \cdot 6H_2O$ to $Mn^{III}(Ac)_3 \cdot 3H_2O$ in the presence of 4-MePy also leads to the same $[Mn^{II}$(L-*mand*)$_2]$ final product.

Complexes Based on Nickel(II) Ion

With the same procedure, it was possible to isolate two 1D chiral nickel(II) polymers: $\{Ni^{II}$(L-*mand*)(4-MePy)$_3\}_n \cdot n(ClO_4)$ [$\mathbf{I_L}$(Ni)] and $\{Ni^{II}$(D-*mand*)(4-MePy)$_3\}_n \cdot n(ClO_4)$ [$\mathbf{I_D}$(Ni)], starting from L- or D-H*mand* ligands, respectively.

Complexes Based on Cobalt(II) Ion

The same procedure under normal atmospheric aerobic conditions gave a black compound. According to single-crystal X-ray measurements, the compound corresponds to the following refined formula: *mer*-$[Co^{III}(4\text{-MePy})_3(N_3)]$ (**II**) with the cobalt ion in a +3 oxidation state and no mandelic ligand (see the Supporting Information for more details). This is in agreement with the observation that the L/D-*mand* ligand has a preference for metal ions in a +2 oxidation state that adopt an octahedral geometry. The presence of azide ion, which is a strong crystal-field ligand, together with aerobic oxidative conditions definitely favored the formation of *mer*-$[Co^{III}(4\text{-MePy})_3(N_3)]$ (**II**). The Co^{III} ion has a slightly distorted octahedral CoN_6 environment formed by coordination of three neutral 4-MePy ligands [Co–N 1.975(2), 1.983(2), 1.966(2) Å] and three azide anions [Co–N 1.953(2), 1.961(2), 1.940(2) Å]. The three azide anions totally compensate the triple positive charge of the Co^{III} ion. By following the same procedure, but under an inert (N_2) atmosphere, it has been effectively possible to isolate the two 1D chiral cobalt(II) compounds as for Ni^{II}, $\{Co^{II}$(L-*mand*)(4-MePy)$_3\}_n \cdot n(ClO_4)$ [$\mathbf{I_L}$(Co)] and $\{Co^{II}$(D-*mand*)(4-MePy)$_3\}_n \cdot n(ClO_4)$ [$\mathbf{I_D}$(Co)].

The role of azide is not thoroughly understood but it is indispensable for the synthesis of the 1D $\mathbf{I_L}$(Ni), $\mathbf{I_L}$(Co), $\mathbf{I_D}$(Ni), and $\mathbf{I_D}$(Co) compounds. The general chemical processes with chiral mandelic acid are illustrated in Scheme 2.

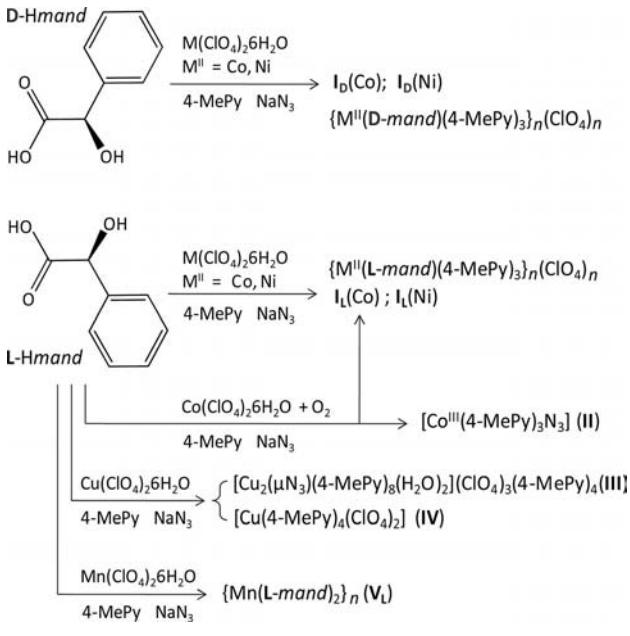

Scheme 2. Chemical transformation in the M^{2+}/NaN_3/mandelic acid system.

Our study focuses on nickel- and cobalt-based chiral 1D polymers with L/D-H*mand* acid. IR, single-crystal X-ray diffraction, circular dichroism, and magnetic properties analyses were performed to thoroughly characterize the stereochemical conformation of the four enantiopure compounds $\mathbf{I_L}$(Ni), $\mathbf{I_L}$(Co), $\mathbf{I_D}$(Ni), and $\mathbf{I_D}$(Co). Details about the nonchiral complexes **II**, **III**, and **IV** in Scheme 2 have been listed in the Supporting Information.

The IR absorption spectra of $\mathbf{I_L}$ and $\mathbf{I_D}$ complexes provide strong evidence for the coordination modes of the carboxylate groups of the α-hydroxycarboxylate ligand (L/D-H*mand*). The $\Delta\nu$ difference between the asymmetric and symmetric stretching frequencies [$\Delta\nu = \nu_{as}(COO^-), -\nu_s(COO^-)$] for the carboxylate ligand is characteristic of a bidentate bridging coordination mode of the carboxylic groups.[40] For example, in the case of the $\mathbf{I_L}$(Ni) IR spectrum, medium intensive bands were found at 1615 cm^{-1}, which are related to $\nu_{as}(COO^-)$, and at 1422 cm^{-1}, which are attributed to $\nu_s(COO^-)$ stretching vibrations. The difference between these two frequencies is equal to 193 cm^{-1} and is characteristic of a bidentate bridging coordination. A strong peak at 1079 cm^{-1} in the IR spectrum of $\mathbf{I_L}$(Ni) indicates the presence of perchlorate anions. Signals [$\nu(CH)_{Py}$ = 3065; ν(CN) = 1592; $\gamma(CH)_{Py}$ = 620 cm^{-1}] for coordinated pyridine rings and for valent oscillations of the ν(OH) group in the range of 3615–2812 cm^{-1} are also present. The latter are large, thus indicating that these –OH groups are most probably involved in strong hydrogen bonds.

The two compounds derived from L-mandelic acid [$\mathbf{I_L}$(Ni), $\mathbf{I_L}$(Co)] are isostructural and exhibit a 1D polymeric structure. The crystallographic independent entity is present in Figure 1 (left side). The refined Flack parameter is equal to –0.02(1) and 0.02(2) for $\mathbf{I_L}$(Ni), $\mathbf{I_L}$(Co), respectively, according to the rules defined in the corresponding part of the Experimental Section. As expected, $\mathbf{I_D}$(Ni) and $\mathbf{I_D}$(Co) structures are the mirror image of $\mathbf{I_L}$(Ni) and $\mathbf{I_L}$(Co), respectively. In those cases, the Flack parameters are equal to 1.00(2) for $\mathbf{I_L}$(Ni) and 0.98(2) for $\mathbf{I_L}$(Co), thereby confirming the existence of the opposite enantiomeric structures.

In all cases ($\mathbf{I_L}$, $\mathbf{I_D}$), the metallic ion (Ni or Co) is located in an N_3O_3 slightly distorted octahedral environment. M–O/N bond lengths range from 2.056 to 2.204 Å (M = Co) and from 2.041 to 2.146 Å (M = Ni) and are in good agreement with those reported previously in the literature.[24–35] It is worth noting that the octahedron in both metal cases is quite regular due to uniform bond lengths and O–M–O bond angles (Tables 1 and 2).

Table 1. Important bond lengths [Å] for the $\mathbf{I_L}$, $\mathbf{I_D}$ complexes.

	$\mathbf{I_L}$(Co)	$\mathbf{I_D}$(Co)	$\mathbf{I_L}$(Ni)	$\mathbf{I_D}$(Ni)
	M = Co		M = Ni	
M1–O1	2.063(2)	2.056(2)	2.041(2)	2.043(2)
M1–O3	2.113(2)	2.109(2)	2.074(2)	2.075(3)
M1–O5	2.146(2)	2.146(2)	2.096(2)	2.093(3)
M1–N21	2.159(2)	2.155(3)	2.112(2)	2.113(3)
M1–N31	2.099(3)	2.099(3)	2.057(2)	2.055(3)
M1–N41	2.204(3)	2.204(2)	2.146(2)	2.139(3)

Table 2. Important bond angles [°] for the $\mathbf{I_L}$, $\mathbf{I_D}$ complexes.

	$\mathbf{I_L}$(Co)	$\mathbf{I_D}$(Co)	$\mathbf{I_L}$(Ni)	$\mathbf{I_D}$(Ni)
	M = Co		M = Ni	
O1–M1–O3	165.86(8)	165.74(8)	169.25(6)	169.4(1)
O1–M1–O5	91.49(9)	91.63(9)	93.20(8)	93.2(1)
O3–M1–O5	75.01(9)	74.81(9)	76.65(8)	76.7(1)
O1–M1–N21	90.4(1)	90.3(1)	89.74(8)	89.7(1)
O3–M1–N21	93.51(9)	93.77(9)	93.46(7)	93.4(1)
O5–M1–N21	88.9(1)	88.8(1)	88.43(8)	88.4(1)
O1–M1–N31	96.67(9)	96.76(9)	93.93(7)	93.9(1)
O3–M1–N31	96.8(1)	96.8(1)	96.34(9)	96.3(1)
O5–M1–N31	171.84(9)	171.60(8)	172.69(7)	172.7(1)
N21–M1–N31	91.2(1)	91.3(1)	89.96(9)	89.9(1)
O1–M1–N41	90.85(9)	90.84(9)	91.21(8)	91.2(1)
O3–M1–N41	85.26(9)	85.07(9)	85.58(7)	85.7(1)
O5–M1–N41	90.8(1)	91.0(1)	91.35(8)	91.4(1)
N21–M1–N41	178.8(1)	178.8(1)	179.03(8)	179.1(1)
N31–M1–N41	88.9(1)	88.8(1)	90.14(8)	90.2(1)

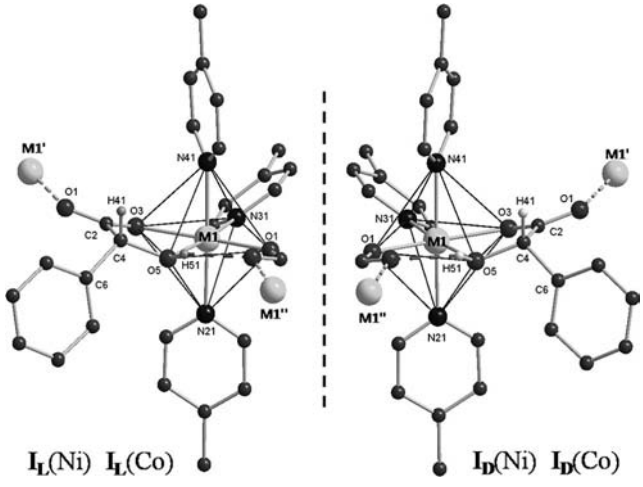

Figure 1. Structure of complexes $\mathbf{I_L}$ and $\mathbf{I_D}$. Hydrogen atoms have been removed for clarity.

The square base of the metal octahedral environment is composed of one nitrogen atom of one methylpyridine (N31) and three oxygen atoms. Two of them belong to one *mand*$^-$ ligand [one (O5) of the hydroxy group and the second one (O3) of the carboxylate entity]. The third oxygen atom (O1) comes from a second *mand*$^-$ ligand. This latter is also connected to a neighboring metal ion to form a polymeric structure (Figure 2). The two apical positions in the octahedral environment are occupied by two nitrogen atoms (N41, N21) from 4-MePy molecules. The H51 hydroxo proton forms a strong intermolecular bond with the oxygen atom (O3) of the carboxylate group along the chain, thereby stabilizing the coordination environments of M^{II}. Similarly (see Scheme 1**D**), the coordination mode of the *mand*$^-$ ligand has already been reported for related compounds.[29–31] The charge of the polymetallic chain is compensated by extra-sphere perchlorate ions and no solvent molecule is present in the crystal packing.

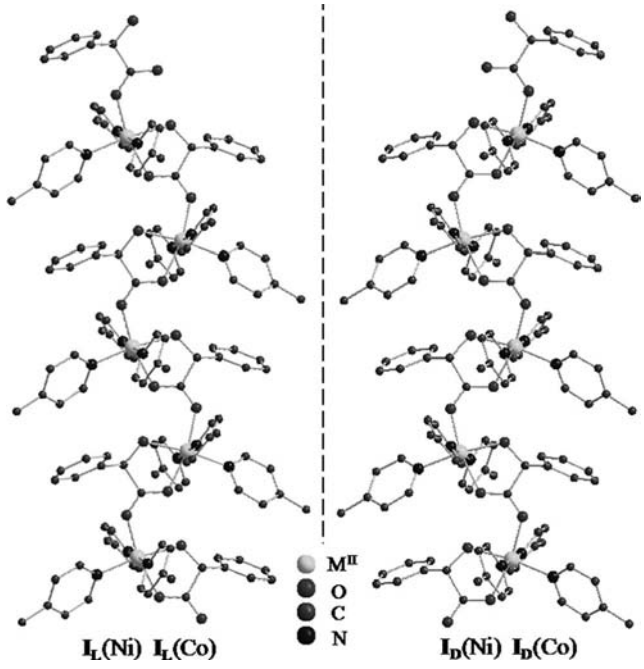

Figure 2. Polymeric chain $\mathbf{I_L}$ and $\mathbf{I_D}$ along the *c* axis of the unit cell. Hydrogen atoms have been removed for clarity.

Chirality in bulk crystals was proven in absorption mode by circular dichroism (CD) spectroscopy in KBr pellets (Figure 3). In the case of cobalt-based chiral polymers, a significant dichroism signature is observed in the 450–629 nm region, which corresponds to the $^4T_{1g}(F) \rightarrow {}^4T_{1g}(P)$ (ν_3) transition of Co^{2+} ions located in an octahedral environment.[31,41–43] The deviation from a symmetric shape of opposite signals in CD spectra between $\mathbf{I_L}$(Co) and $\mathbf{I_D}$(Co) is likely to be related to uncertainties in the background correction because the latter is very sensitive to small differences in the thickness and transparency of KBr pellets. Unfortunately, the presence of perchlorate ions in these compounds does not allow one to apply the strong pressure that is indispensable to fabricating KBr pellets of good quality. However, this study clearly indicates that the two cobalt-based enantiomers exhibit similar but opposite signals, thus demonstrating the homochiral nature of their structure.

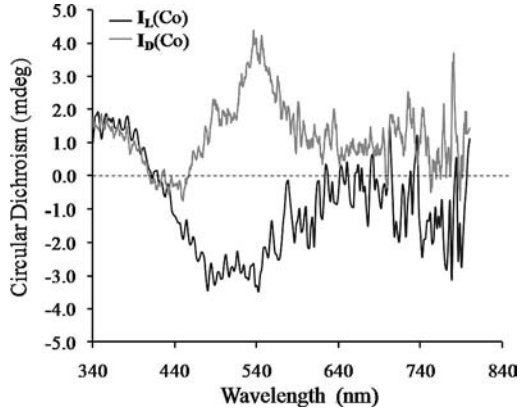

Figure 3. CD spectra of $\mathbf{I_L}$(Co) and $\mathbf{I_D}$(Co) in KBr.

The temperature dependence of the magnetic susceptibility of complexes $\mathbf{I_L}$(Ni), $\mathbf{I_L}$(Co), $\mathbf{I_D}$(Ni), and $\mathbf{I_D}$(Co) has been measured in the temperature range of 2–300 K under a magnetic field of 0.1 T, as shown in Figure 4 (see also Figure S6 in the Supporting Information). For nickel(II)-based compounds [$\mathbf{I_L}$(Ni) and $\mathbf{I_D}$(Ni)], the χT product per Ni^{II} atom at room temperature is equal to 1.21 and 1.20 $cm^3 K mol^{-1}$, respectively. As generally observed for nickel(II) complexes, these values are larger than the spin-only value of 1.0 $cm^3 K mol^{-1}$ for uncoupled Ni^{II} with S = 1 and g = 2.00. A gradual increase in χT is observed on cooling to reach values equal to 1.40 and 1.38 $cm^3 K mol^{-1}$, respectively, at 5 K. This behavior is characteristic of ferromagnetic interactions for complexes $\mathbf{I_L}$(Ni) and $\mathbf{I_D}$(Ni). Below 5 K, in both cases, the χT product decreases to 1.14 $cm^3 K mol^{-1}$ at 2 K, thus suggesting the presence of intermolecular interactions or the effect of zero-field splitting (ZFS) that is characteristic of octahedral Ni^{II} ion with S = 1 in $^3T_{2g}$ configuration.[44] The magnetic susceptibility obeys the Curie–Weiss law with positive Weiss constants θ

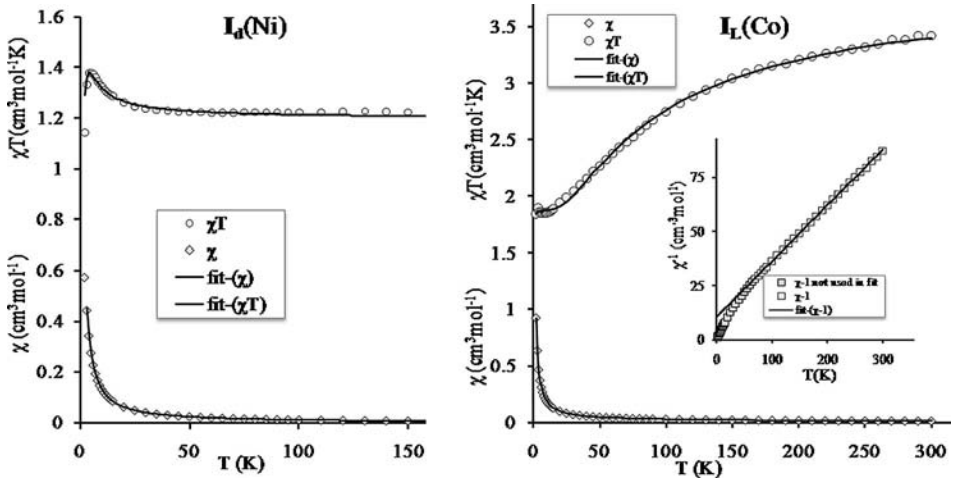

Figure 4. χT and χ versus T plots data for $\mathbf{I_D}$(Ni) (left) and χT, χ, and χ^{-1} versus T plots for $\mathbf{I_L}$(Co) (right) per M^{II} atom. The solid lines correspond to the best fit with models and parameters indicated in the text.

= 0.5(1) K [1.25(2) for $\mathbf{I_D}$(Ni)] and Curie constant C = 1.19 $cm^3 K mol^{-1}$ [1.20(2) for $\mathbf{I_D}$(Ni)]. This confirms the presence of ferromagnetic interactions in these complexes. The Curie constant gives a factor g = 2.18 calculated with $C = \frac{Ng^2\beta^2}{3k}S(S+1)$ in which S = 1.

Different models (1–4) have been tested to estimate the strength of the magnetic interaction in the S = 1 ferromagnetic nickel-based chain and to estimate the zero-field splitting contribution.

The first tested model, Model 1, has been developed by Fisher[45] assuming Heisenberg interactions between spins within the chain with well-known Fisher formula:

$$\chi = \frac{\beta N_A \mu_B^2 g^2 S(S+1)}{3kT}\cdot\frac{1+u}{1-u}$$

$$u = \coth((jS(S+1)/kT) - (kT/(jS(S+1)))$$

This model has been predominantly used for isotropic S = 5/2 systems (see, for example, the literature[46,47]) but also to characterize Ni^{II} chains with antiferromagnetic[48–50] or ferromagnetic[51] exchange interactions. The magnetic behaviors of $\mathbf{I_L}$(Ni) and $\mathbf{I_D}$(Ni) compounds have been fitted using this model and by taking into account an intermolecular interaction term (zJ') and an impurities contribution (ρ). The best fits are presented in the Supporting Information, and resulting parameters are given in Table 3. The small ferromagnetic interactions, +1.71 and +1.49 cm^{-1} obtained for $\mathbf{I_L}$(Ni) and $\mathbf{I_D}$(Ni), respectively, correspond to the magnetic interaction between Ni^{II} cations located in an octahedral environment.

The second model, Model 2, is based on the equation that has been developed by Monfort et al. for alternate ferromagnetic S = 1 chains.[52] This model uses the isotropic Hamiltonian:

$$H = -\sum_{i=1}^{N-1}\left[2J_1 S_{2i} S_{2i+1} + 2J_2 S_{2i} S_{2i-1}\right]$$

in which $J_1 = J_2 = J$ and was also used for the characterization of Ni^{II} ferromagnetic chains:[46,52,53]

$$\chi = \frac{2Ng^2\beta^2}{3kT}\cdot\frac{Ax^3 + Bx^2 + Cx + 1}{Dx^2 + Ex + 1}$$

in which A = 0.14709, B = –0.788967, C = 0.866426, D = 0.096573, E = –0.624929, and $x = \frac{J}{kT}$. As for Model 1, interchain magnetic interactions (zJ') and paramagnetic impurities (ρ) were included.

The best fit of the experimental data (2–300 K, Table 4, Figure S6 in the Supporting Information) gave for the interaction (J) +1.67(9) and +1.39(4) cm^{-1} for $\mathbf{I_L}$(Ni) and $\mathbf{I_D}$(Ni), respectively, which confirms the ferromagnetic interactions along the chain.

Table 3. Best parameters obtained from magnetic-susceptibility data fitting.

	Model 1[43]		Model 2[50]		Model 3[52]		Model 4[56]	
	$\mathbf{I_L}$(Ni)	$\mathbf{I_D}$(Ni)	$\mathbf{I_L}$(Ni)	$\mathbf{I_D}$(Ni)	$\mathbf{I_L}$(Ni)	$\mathbf{I_D}$(Ni)	$\mathbf{I_L}$(Ni)	$\mathbf{I_D}$(Ni)
J [cm^{-1}]	1.71(6)	1.49(2)	1.67(9)	1.39(4)	2.3(1)	1.98(5)	0.64(5)	0.54(7)
D [cm^{-1}]							–1.38(1)	–1.05(2)
g	2.145(5)	2.187(2)	2.132(6)	2.178(4)	2.135(6)	2.180(3)	2.165(3)	2.190(4)
zJ [cm^{-1}]	–0.77(2)	–0.78(1)	–0.64(2)	–0.65(1)	–0.65(2)	–0.66(1)	–0.3(4)	–0.4(5)
ρ [%]	1.3(3)	0.3(1)	1.7(4)	0.5(2)	1.7(3)	0.5(2)	–	–

Table 4. Single-crystal X-ray data collection details and refinement results.

	$\mathbf{I_L}$(Co)	$\mathbf{I_D}$(Co)	$\mathbf{I_L}$(Ni)	$\mathbf{I_D}$(Ni)
Empirical formula	$C_{26}H_{28}ClCoN_3O_7$	$C_{26}H_{28}ClCoN_3O_7$	$C_{26}H_{28}ClNiN_3O_7$	$C_{26}H_{28}ClNiN_3O_7$
M_r [$g mol^{-1}$]	588.9	588.9	588.7	588.7
Crystal system	orthorhombic	orthorhombic	orthorhombic	orthorhombic
Space group	$P2_12_12_1$	$P2_12_12_1$	$P2_12_12_1$	$P2_12_12_1$
a [Å]	9.7822(2)	9.7495(2)	9.6643(7)	9.6741(5)
b [Å]	12.5962(3)	12.6069(3)	12.7173(7)	12.6754(7)
c [Å]	22.6256(4)	22.5939(5)	22.375(1)	22.3954(9)
V [$Å^3$]	2787.9(1)	2777.0(3)	2750.0(4)	2746.2(3)
Z	4	4	4	4
T [K]	293	293	293	293
D [$g cm^{-3}$]	1.403	1.408	1.422	1.424
μ [mm^{-1}]	0.759	0.762	0.851	0.852
F(000)	1220	1220	1224	1224
Independent reflections	3709	3614	6466	3551
R_{int}	0.035	0.033	0.045	0.044
$R(F)/R_w(F)$	0.0309/0.0336	0.0309/0.0342	0.0347/0.0348	0.0316/0.0340
S	1.13	1.13	0.99	1.13
Reflections	3801	3685	5286	3327
Parameters	344	344	344	344
$\Delta\rho_{max}/\Delta\rho_{min}$ [$e Å^{-3}$]	0.28/–0.21	0.33/–0.21	0.29/–0.34	0.31/–0.23
Absorption correction	multiscan	multiscan	analytical	multiscan
Flack parameter	0.02(2)	0.98(2)	–0.02(1)	1.00(2)

The third model, Model 3, is a recent approach that has been developed by M. Drillon on the basis of a noncritical scaling model to describe the behavior of low-dimensional magnetic systems.[54] This model was previously used to characterize Cu^{II} and Ni^{II} chains[55–57] by using the analytical expression:

$$\chi = \frac{2Ng^2\beta^2}{3kT}\cdot S(S+1)\cdot\left(1+\frac{0.61J(S+1)}{kT}\right)^{1.23S}$$

Using this model, good agreements between the experimental data and the simulated one have been obtained for both nickel [$\mathbf{I_L}$(Ni) and $\mathbf{I_D}$(Ni)] chains, thereby confirming the ferromagnetic interactions along the chain (see Table 3 and Figure S6 in the Supporting Information).

The last model tested to discuss the magnetic behavior of our chiral 1D polymers, Model 4, has been proposed by Neef for the characterization of an $S = 1$ ferromagnetic chain with ZFS and is based on the Hamiltonian:[53,58,59]

$$H = -2J\sum_{i=1}^{N}(S_iS_{i+1}) - D\sum_{i=1}^{N}\left[S_{iz}^2 - \tfrac{2}{3}\right]$$

in which J is the constant of magnetic interaction along the chain, and D is the single-ion zero-field splitting factor of Ni^{II}. The fitted parameters of the equation for the ferromagnetic Ni^{II} chain by Neef model are the following:

$$\chi = \frac{2Ng^2\beta^2}{kT(2+e^{-y})} + \frac{Ng^2\beta^2}{kT}F_1 + \frac{Ng^2\beta^2}{3kT}F_2$$

in which $x = \frac{J}{kT}$, $y = \frac{D}{kT}$, $F_1 = 0.6666 + 1.7778x + 1.4815x^2 - 1.5802x^3 - 2.1399x^4 + 5.3728x^5$, $F_2 = -2 + 3.5555xy + 6.2222x^2y + 1.9753x^3y - 6.2222x^4y - 0.43018x^5y + 1.9259x^2y^2 + 5.9918x^3y^2 + 3.5084x^4y^2 - 0.39506xy^3 - 0.872243x^2y^3 + 0.55748x^3y^3 + 0.032922xy^4 - 0.31358x^2y^4 + 0.04609xy^5$. Using the above expression, the best fit of the magnetic-susceptibility behavior (2–300 K) is obtained with the following parameters $J = 0.64(5)$ cm^{-1}, $g = 2.165(3)$, $D = -1.38(1)$ cm^{-1} for $\mathbf{I_L}$(Ni) and $J = 0.54(7)$ cm^{-1}, $g = 2.190(4)$, $D = -1.05(2)$ cm^{-1} for $\mathbf{I_D}$(Ni).

The obtained g value is in good agreement with what was obtained in the case of Curie constants, and the J value that corresponds to the ferromagnetic interaction is moderately lower but still comparable to those from models presented above. Magnetization curves per Ni atoms show deviation from Brillouin behavior, and this phenomenon could be due to ZFS or small ferromagnetic interactions along the chain. Ac-susceptibility measurements were carried out for both $\mathbf{I_L}$(Ni) and $\mathbf{I_D}$(Ni); however, there was no increase in the out-of-phase χ' signal down to 2 K and up to 1400 Hz. The non-appearance of a χ'' signal for $\mathbf{I_L}$(Ni) and $\mathbf{I_D}$(Ni) suggests the absence of long-range ordering process at measured temperatures (2–26 K).

In the case of the isostructural cobalt(II) compounds, the decay of χT upon cooling is shown in Figure 4 (see also Figure S7 in the Supporting Information). The χT product per Co^{II} at room temperature is 3.43 and 3.37 cm^3 K mol^{-1} for $\mathbf{I_L}$(Co) and $\mathbf{I_D}$(Co), respectively. The value of χT is larger than the spin-only 1.87 cm^3 K mol^{-1} for the $S = 3/2$ with $g = 2.00$ and suggests the presence of an important spin–orbital contribution that is characteristic of octahedral high-spin Co^{II}. A gradual decrease in χT is observed with temperature; χT reaches values of 1.85 and 1.78 cm^3 K mol^{-1} at 8 K and slowly goes up in the 8–2 K temperature region (Figure 3). The magnetic behavior of $\mathbf{I_D}$(Co) is similar to $\mathbf{I_L}$(Co) (in limit-of-error experiments) and is dominated by a strong spin–orbital contribution characteristic of octahedral Co^{II}. It is worth noting here that it seems to validate the potential presence of small ferromagnetic interactions along the chain. Similar small ferromagnetic interactions between octahedral Co^{II} centers through a bridged carboxylic group have been recently reported in the literature.[31,43,55] To get an estimated value for exchange interactions, a simple model that involves the spin–orbit coupling and the exponential low-temperature divergence of the susceptibility [$\chi T \propto \exp(+J/2kT)$] of an Ising chain of anisotropic magnetic centers can be used.[31,55,60,61] Two contributions are included in the equation:

$$\chi = \frac{A_1}{T}\exp\left(-\frac{E_1}{kT}\right) + \frac{A_2}{T}\exp\left(-\frac{E_2}{kT}\right)$$

in which $A_1 + A_2$ is equal to the Curie constant, and the limiting Curie–Weiss equation $\chi = \frac{A_1 + A_2}{T - \theta}$ was applied to constrain the fitting procedure. E_1 and E_2 are the activation energies that correspond to the spin–orbit coupling and to the ferromagnetic exchange interaction, respectively.

The three sets of experimental data (χ, χT, χ^{-1}) for $\mathbf{I_L}$(Co) and $\mathbf{I_D}$(Co) have been simultaneously fitted by using a nonlinear least-squares method.

The best fit was obtained for parameters $\mathbf{I_L}$(Co) $A_1 = 2.01(4)$ cm^3 K mol^{-1}, $E_1 = 56(2)$ cm^{-1}, $A_2 = 1.88(4)$ cm^3 K mol^{-1}, $E_2 = 0.02(7)$ cm^{-1}, $\theta = -1.322(6)$ K, and $\mathbf{I_D}$(Co) $A_1 = 1.97(4)$ cm^3 K mol^{-1}, $E_1 = 52(2)$ cm^{-1}, $A_2 = 1.82(4)$ cm^3 K mol^{-1}, $E_2 = 0.02(7)$ cm^{-1}, $\theta = -1.264(6)$ K. The obtained parameters A_1 and A_2 are in good agreement with those previously reported for Co^{II} carboxylates, and the sum of A_1 and A_2 represent the Curie constant.[62] The E_1 parameters are consistent with those reported in the literature (E_1/k in the range of 50–100 K) and reflect the spin–orbital coupling and distortion in octahedral Co^{II}.[31,43,55,63,64] The E_2 parameter reflects the very small ferromagnetic interaction (0.02 cm^{-1}) within the Ising chain approximation.

Magnetization curves for compounds $\mathbf{I_L}$(Co) and $\mathbf{I_D}$(Co) with saturation values of 2.31 M.B. and 2.35 M.B. at 5 T are consistent with the values expected for a noninteracted mononuclear Co^{II} compound.[65–69]

Conclusion

Four new isomorphic coordination polymers have been synthesized and fully characterized. Within the chains, divalent metal ions, Co^{II} or Ni^{II}, are linked by a chiral mandelic acid (D or L). X-ray analyses show non-centrosymmet-

ric (orthorhombic, $P2_12_12_1$) structural organizations with refined Flack parameters close to 0 or 1 for the L or D isomer, respectively. The chirality of bulk materials was also proven by circular dichroism spectroscopy in the solid state. Magnetic studies on Ni^{II} and Co^{II} compounds reveal that the carboxylate bridge transmits ferromagnetic coupling along the chains. Ferromagnetic coupling in the chiral Ni^{II}-based polymer are similar in the two optical isomers [0.64(5)/0.54(7) cm^{-1}] with similar ZFS parameters [–1.38(1)/–1.05(2) cm^{-1}]. In the case of the Co^{II}-based polymer, negligible ferromagnetic interaction is suspected.

Experimental Section

General: All starting materials and solvents were purchased from Aldrich and were used without further purification. IR spectra were recorded with a GX system 2000 Perkin–Elmer spectrophotometer and samples were run as KBr pellets.

The circular dichroism (CD) spectra were recorded with a Chirascan spectropolarimeter using Chirascan software (Applied Biophysics Ltd., Leatherhead, UK) in KBr pellets.

Synthesis of $\mathbf{I_L}$(Ni): A mixture of $Ni(ClO_4)_2{\cdot}6H_2O$ (2 mmol, 0.74 g), L-mandelic acid (2 mmol, 0.30 g), and sodium azide (2 mmol 0.13 g) in methanol (80 mL) was stirred for 10 min at room temperature. Then 4-MePy (2 mL) was added. In the following days, slow evaporation of the solution at room temperature yielded blue crystals of $\mathbf{I_L}$(Ni); yield 56% based on Ni. $C_{26}H_{28}ClN_3NiO_7$ (588.7): calcd. C 53.05, H 4.79, N 7.14; found C 52.85, H 4.91, N 7.10.

The synthesis of $\mathbf{I_D}$(Ni) was identical to that of $\mathbf{I_L}$(Ni); yield 51% based on Ni. $C_{26}H_{28}ClN_3NiO_7$ (588.7): calcd. C 53.05, H 4.79, N 7.14; found C 52.79, H 4.93, N 7.09.

Synthesis of $\mathbf{I_L}$(Co) and $\mathbf{I_D}$(Co): A procedure similar to $\mathbf{I_L}$(Ni) was followed to prepare cobalt(II) compounds except $Ni(ClO_4)_2{\cdot}6H_2O$ was replaced by $Co(ClO_4)_2{\cdot}6H_2O$ (2 mmol, 0.75 g). The final product was contaminated by crystals of mononuclear compound *mer*-$[Co^{III}(4\text{-}MePy)_3(N_3)]$ (**II**), which were separated off and characterized by single-crystal X-ray analysis. To obtain pure samples of $\mathbf{I_L}$(Co) and $\mathbf{I_D}$(Co), the synthesis were performed in a similar manner but under an inert atmosphere (N_2) to prevent oxidation process of Co^{II}. In the following days, slow evaporation of the solution at room temperature yielded reddish crystals of $\mathbf{I_L}$(Co); yield 43% based on Co. $C_{26}H_{28}ClCoN_3O_7$ (588.9): calcd. C 53.03, H 4.79, N 7.14; found C 52.95, H 4.89, N 7.08. $\mathbf{I_D}$(Co): Yield 45% based on Co. $C_{26}H_{28}ClCoN_3O_7$ (588.9): calcd. C 53.03, H 4.79, N 7.14; found C 52.91, H 4.83, N 7.11.

A similar synthetic procedure was used with the Mn^{II} and Cu^{II} perchlorate salts. According to the elemental analysis, IR spectra, and powder X-ray analyses, the resulting compounds correspond to those characterized and reported previously.[29–31]

In the case of synthesis with Cu^{II} salts, we obtained the oil with a two type of crystals (**III** and **IV**), which were sorted out manually for IR and single-crystal X-ray analyses. According to X-ray analyses, the compositions corresponded to $[Cu_2(\mu\text{-}N_3)(4\text{-}MePy)_8(H_2O)_2](ClO_4)_3(4\text{-}MePy)_4$ (**III**) and $[Cu(4\text{-}MePy)_4(ClO_4)_2]$ (**IV**).

Magnetic Measurements: Magnetic-susceptibility data (2–300 K) were collected on powdered polycrystalline samples by a Quantum Design MPMS SQUID magnetometer and under an applied magnetic field of 0.1 T. The magnetization isotherm was collected at 2 K between 0 and 5 T. All data were corrected for the contribution of the sample holder and diamagnetism of the samples estimated with Pascal's constants.[64,70] The analysis of magnetic data was carried out by simulation of $\chi T(T)$ and $\chi(T)$ thermal dependences including impurities contribution (ρ) and intermolecular interactions (zJ') according to the following expression:

$$\chi(T)=\frac{\chi(T)}{\left[1-\frac{2zJ'\chi(T)}{Ng^2\beta^2}\right]}(1-\rho)+\rho\frac{Ng^2\beta^2}{3kT}S(S+1)$$

The theoretical magnetic susceptibility of $\chi T(T)$ and $\chi(T)$ has been obtained by models exposed further in the text. Minimization was carried out with an adapted version of Visualiseur–Optimiseur for Matlab[71,72] using nonlinear least-squares by the Lavenberg–Marquard[73] algorithm.

X-ray Analysis: It was possible to determine by single-crystal X-ray diffraction the structure of four original 1D polymer metal complexes. CCDC-824526 [for $\mathbf{I_L}$(Co)], -824527 [for $\mathbf{I_D}$(Co)], -824528 [for $\mathbf{I_L}$(Ni)], -824529 [for $\mathbf{I_D}$(Ni)], -824530 (for **III**), -824531 (for **IV**), and -824532 (for **II**) contain the supplementary crystallographic data for this paper. These data can be obtained free of charge from The Cambridge Crystallographic Data Centre via www.ccdc.cam.ac.uk/data_request/cif.

Diffraction data sets were collected with a Gemini Oxford diffractometer equipped with a CCD camera and by using the related software.[74] A semiempirical absorption correction (multiscan) has been applied to all the data sets.[75] All the structures were solved by direct methods using the SIR97 program[76] combined with Fourier difference syntheses and refined against F using the CRYSTALS program.[77] In each structure, all atomic displacements for non-hydrogen atoms were refined with an anisotropic model. Hydrogen atoms have been placed by Fourier. Differences account for the hybridization of the supporting atoms and for the possible presence of hydrogen bonds in the case of donor atoms.

All hydrogen atoms have been refined using a riding mode. The structures have been solved and refined using a non-centrosymmetric space group (orthorhombic, $P2_12_12_1$). The Flack parameter[78] has been refined for all structures by keeping the same atom-position structural model and is then equal either to 0 or 1. This preconception has been chosen to clearly demonstrate the obtaining of pure opposite enantiomeric complexes for cobalt(II) and nickel(II). X-ray crystallographic data and refinement details for compounds named $\mathbf{I_L}$(Co), $\mathbf{I_D}$(Co), $\mathbf{I_L}$(Ni), and $\mathbf{I_D}$(Ni) are summarized in Table 4. Important bond lengths and angles are presented in Table 1 and Table 2, respectively.

Supporting Information (see footnote on the first page of this article): X-ray data collection details and plots of the structures of compounds **II**, **III**, **IV**. Fit of magnetic susceptibilities for $\mathbf{I_L}$(Ni) and $\mathbf{I_D}$(Ni) using models 1–4, magnetization plots for investigated compounds, and IR spectra.

Acknowledgments

G. N. thanks the Marie Curie Actions (FP7-People-IIF) for financial support.

[1] M. J. Zaworotko, *Chem. Soc. Rev.* **1994**, *23*, 283–288.
[2] B. Moulton, M. J. Zaworotko, *Chem. Rev.* **2001**, *101*, 1629–1658.
[3] M. Dinca, J. R. Long, *Angew. Chem.* **2008**, *120*, 6870; *Angew. Chem. Int. Ed.* **2008**, *47*, 6766–6779.

[4] L. J. Murray, M. Dinca, J. R. Long, *Chem. Soc. Rev.* **2009**, *38*, 1294–1314.
[5] P. Dechambenoit, J. R. Long, *Chem. Soc. Rev.* **2011**, *40*, 3249–3265.
[6] P. Amo-Ochoa, R. Jimenez-Aparicio, M. R. Torres, F. A. Urbanos, A. Gallego, C. J. Gomez-Garcia, *Eur. J. Inorg. Chem.* **2010**, 4924–4932.
[7] W. Kaim, M. Moscherosch, *Coord. Chem. Rev.* **1994**, *129*, 157–193.
[8] B. L. Chen, S. C. Xiang, G. D. Qian, *Acc. Chem. Res.* **2010**, *43*, 1115–1124.
[9] M. P. Suh, Y. E. Cheon, E. Y. Lee, *Coord. Chem. Rev.* **2008**, *252*, 1007–1026.
[10] M. W. Hosseini, *Coord. Chem. Rev.* **2005**, *38*, 313–323.
[11] M. W. Hosseini, *Coord. Chem. Rev.* **2003**, *240*, 157–166.
[12] D. C. Sherrington, K. A. Taskinen, *Chem. Soc. Rev.* **2001**, *30*, 83–93.
[13] H. W. Roesky, M. Andruh, *Coord. Chem. Rev.* **2003**, *236*, 91–119.
[14] M. Oh, G. B. Carpenter, D. A. Sweigart, *Coord. Chem. Rev.* **2004**, *37*, 1–11.
[15] M. H. Filby, J. W. Steed, *Coord. Chem. Rev.* **2006**, *250*, 3200–3218.
[16] K. M. Fromm, *Coord. Chem. Rev.* **2008**, *252*, 856–885.
[17] R. M. Yu, X. F. Kuang, X. Y. Wu, C. Z. Lu, J. P. Donahue, *Coord. Chem. Rev.* **2009**, *253*, 28722–890.
[18] H. Kumagai, K. Inoue, *Angew. Chem.* **1999**, *111*, 1694; *Angew. Chem. Int. Ed.* **1999**, *38*, 1601–1603.
[19] Y. Numata, K. Inoue, N. Baranov, M. Kurmoo, K. Kikuchi, *J. Am. Chem. Soc.* **2007**, *129*, 9902–9909.
[20] M. Minguet, D. Luneau, E. Lhotel, V. Villar, C. Paulsen, D. B. Amabilino, J. Veciana, *Angew. Chem.* **2002**, *114*, 606; *Angew. Chem. Int. Ed.* **2002**, *41*, 586–589.
[21] E. Lhotel, D. B. Amabilino, C. Sporer, D. Luneau, J. Veciana, C. Paulsen, *Phys. Rev. B* **2008**, *77*, 064416, 1–8.
[22] C. Train, R. Gheorghe, V. Krstic, L. M. Chamoreau, N. S. Ovanesyan, G. Rikken, M. Gruselle, M. Verdaguer, *Nat. Mater.* **2008**, *7*, 729–734.
[23] C. Train, T. Nuida, R. Gheorghe, M. Gruselle, S. Ohkoshi, *J. Am. Chem. Soc.* **2009**, *131*, 16838–16843.
[24] D. A. House, J. Browning, J. R. Pipal, W. T. Robinson, *Inorg. Chim. Acta* **1999**, *292*, 73–83.
[25] R. Carballo, A. Castineiras, S. Balboa, B. Covelo, J. Niclos, *Polyhedron* **2002**, *21*, 2811–2818.
[26] R. Carballo, B. Covelo, S. Balboa, A. Castineiras, J. Niclos, *Z. Anorg. Allg. Chem.* **2001**, *627*, 948–954.
[27] R. Carballo, B. Covelo, E. M. Vazquez-Lopez, E. Garcia-Martinez, A. Castineiras, J. Niclos, *Z. Anorg. Allg. Chem.* **2005**, *631*, 785–792.
[28] R. Carballo, A. Castineiras, B. Covelo, E. Garcia-Martinez, J. Niclos, E. M. Vazquez-Lopez, *Polyhedron* **2004**, *23*, 1505–1518.
[29] H. Kumagai, Y. Oka, K. Inoue, M. Kurmoo, *J. Phys. Chem. Solids* **2004**, *65*, 55–60.
[30] A. Beghidja, S. Hallynek, R. Welter, P. Rabu, *Eur. J. Inorg. Chem.* **2005**, 662–669.
[31] A. Beghidja, G. Rogez, P. Rabu, R. Welter, M. Drillon, *J. Mater. Chem.* **2006**, *16*, 2715–2728.
[32] B. Schetter, C. Stosiek, B. Ziemer, R. Mahrwald, *Appl. Organomet. Chem.* **2007**, *21*, 139–145.
[33] M. Ahmed, P. Schwendt, J. Marek, M. Sivak, *Polyhedron* **2004**, *23*, 655–663.
[34] I. K. Smatanova, J. Marek, P. Svancarek, P. Schwendt, *Acta Crystallogr., Sect. C: Crys. Str. Commun.* **2000**, *56*, 154–155.
[35] M. H. Zeng, S. Gao, X. M. Chen, *Inorg. Chem. Commun.* **2004**, *7*, 864–867.
[36] D. A. Evans, K. A. Woerpel, M. J. Scott, *Angew. Chem.* **1992**, *104*, 439; *Angew. Chem. Int. Ed. Engl.* **1992**, *31*, 430–432.
[37] A. J. Blake, N. R. Champness, P. A. Cooke, J. E. B. Nicolson, C. Wilson, *J. Chem. Soc., Dalton Trans.* **2000**, 3811–3819.
[38] Z. J. Lin, A. M. Z. Slawin, R. E. Morris, *J. Am. Chem. Soc.* **2007**, *129*, 4880–4881.
[39] F. Cotton, G. Wilkinson, C. Murillo, C. Murillo, M. Bochmann, *Adv. Inorg. Chem. Vol. 706*, Wiley, New York, **1999**.
[40] K. Nakamoto, *Infrared and Raman Spectra of Inorganic and Coordination Compound*, 5th ed., Wiley, **1997**.
[41] L. I. Katzin, *Inorg. Chem.* **1973**, *12*, 649–655.
[42] C. Livage, N. Guillou, P. Rabu, P. Pattison, J. Marrot, G. Ferey, *Chem. Commun.* **2009**, 4551–4553.
[43] A. Beghidja, P. Rabu, G. Rogez, R. Welter, *Chem. Eur. J.* **2006**, *12*, 7627–7638.
[44] R. Boca, *Coord. Chem. Rev.* **2004**, *248*, 757–815.
[45] M. E. Fisher, *Am. J. Phys.* **1964**, *32*, 343.
[46] Y. Ma, J. Y. Zhang, A. L. Cheng, Q. Sun, E. Q. Gao, C. M. Liu, *Inorg. Chem.* **2009**, *48*, 6142–9082.
[47] R. Herchel, Z. Sindelar, Z. Travnicek, R. Zboril, J. Vanco, *Dalton Trans.* **2009**, 9870–287.
[48] M. M. Morelock, M. L. Good, L. M. Trefonas, D. Karraker, L. Maleki, H. R. Eichelberger, R. Majeste, J. Dodge, *J. Am. Chem. Soc.* **1979**, *101*, 4858–4866.
[49] K. Y. Choi, K. J. Kim, *Polyhedron* **2008**, *27*, 1310–3526.
[50] W. Ouelleffe, A. V. Prosvirin, J. Valeich, K. R. Dunbar, J. Zubieta, *Inorg. Chem.* **2007**, *46*, 9067–9082.
[51] H. Z. Kou, S. F. Si, S. Gao, D. Z. Liao, Z. H. Jiang, S. P. Yan, Y. G. Fan, G. L. Wang, *Eur. J. Inorg. Chem.* **2002**, 699–702.
[52] M. Monfort, I. Resino, M. S. El Fallah, J. Ribas, X. Solans, M. Font-Bardia, H. Stoeckli-Evans, *Chem. Eur. J.* **2001**, *7*, 280–287.
[53] Y. Ma, A. L. Cheng, E. Q. Gao, *Dalton Trans.* **2010**, *39*, 3521–3526.
[54] J. Souletie, P. Rabu, M. Drillon, *Phys. Rev. B* **2005**, *72*.
[55] A. Beghidja, R. Welter, P. Rabu, G. Rogez, *Inorg. Chim. Acta* **2007**, *360*, 1111–1120.
[56] G. Chastanet, B. Le Guennic, C. Aronica, G. Pilet, D. Luneau, M. L. Bonnet, V. Robert, *Inorg. Chim. Acta* **2008**, *361*, 3847–3855.
[57] E. M. Bauer, C. Bellitto, G. Righini, M. Colapietro, G. Portalone, M. Drillon, P. Rabu, *Inorg. Chem.* **2008**, *47*, 10945–10952.
[58] D. T. Neef, *PhD Thesis*, Eindhoven (The Netherlands), **1975**.
[59] J. Ribas, M. Monfort, B. K. Ghosh, R. Cortes, X. Solans, M. FontBardia, *Inorg. Chem.* **1996**, *35*, 864–868.
[60] L. A. Barrios, J. Ribas, G. Aromi, *Inorg. Chem.* **2007**, *46*, 7154–7162.
[61] H. S. Yoo, J. I. Kim, N. Yang, E. K. Koh, J. G. Park, C. S. Hong, *Inorg. Chem.* **2007**, *46*, 9054–9056.
[62] W. K. Robinson, S. A. Friedberg, *Phys. Rev.* **1960**, *117*, 402–408.
[63] R. Carlin, *Magnetochemistry*, Springer Verlag, **1986**.
[64] O. Kahn, *Molecular Magnetism*, VCH, New York, Weinheim, Cambridge, **1993**.
[65] Y. Oka, K. Inoue, *Chem. Lett.* **2004**, *33*, 402–403.
[66] B. Zurowska, A. Brzuszkiewicz, *Polyhedron* **2008**, *27*, 1623–1630.
[67] H. Jankovics, M. Daskalakis, C. P. Raptopoulou, A. Terzis, V. Tangoulis, J. Giapintzakis, T. Kiss, A. Salifoglou, *Inorg. Chem.* **2002**, *41*, 3366–3374.
[68] B. Papankova, R. Boca, L. Dlhan, I. Nemec, J. Titis, I. Svoboda, H. Fuess, *Inorg. Chim. Acta* **2010**, *363*, 147–156.
[69] M. Menelaou, A. Konstantopai, C. Mateescu, H. Zhao, C. Drouza, N. Lalioti, A. Salifoglou, *Inorg. Chem.* **2009**, *48*, 8092–8105.
[70] P. Pascal, *Ann. Chim. Phys.* **1910**, *19*, 5.
[71] *MATLAB*, The MathWorks Inc., **2000**.
[72] F. Yerly, *VISUALISEUR-OPTIMISEUR*, EPFL, Lausanne, **2003**.
[73] J. Nocedal, S. Wright, *Numerical Optimization*, 2nd ed., Springer, **2006**.
[74] *CrysAlisPro*, version 1.171.34.40 (rel. 27-08-2010, CrysAlis171. NET), Oxford Diffraction Ltd..

[75] O. D. L. CrysAlisPro, Version 1.171.34.40 (rel. 27-08-2010, CrysAlis171.NET), (compiled Aug. 27, 2010, 11:50:40). Analytical numeric absorption correction using a multifaceted crystal model based on expressions derived by: R. C. Clark, J. S. Reid, *Acta Crystallogr., Sect. A* **1995**, *51*, 887–897.
[76] G. Cascarano, A. Altomare, C. Giacovazzo, A. Guagliardi, A. G. G. Moliterni, D. Siliqi, M. C. Burla, G. Polidori, M. Camalli, *Acta Crystallogr., Sect. A* **1966**, *52*, C79.
[77] D. Watkin, C. Prout, J. Carruthers, P. Betteridge, *Chemical Crystallography Laboratory*, Oxford, UK, **1999**.
[78] H. Flack, *Acta Crystallogr., Sect. A: Foundations of Crystallography* **1983**, *39*, 876–881.

Received: May 25, 2011
Published Online: September 14, 2011

